PERGAMON

International Journal of Solids and Structures 38 (2001) 1791–1811

INTERNATIONAL JOURNAL OF SOLIDS and STRUCTURES

www.elsevier.com/locate/ijsolstr

A review of analytical aspects of fretting fatigue, with extension to damage parameters, and application to dovetail joints ☆

M. Ciavarella [a,*], G. Demelio [b]

[a] CNR-IRIS, COMES Computational Mechanics of Solids, Str. Crocefisso 2/B, 70126 Bari, Italy
[b] DPPI – Politecnico di Bari, v.le Gentile 182, 70126 Bari, Italy

Received 2 September 1999; in revised form 10 February 2000

Abstract

Recent advances by the authors in analytical methods for the analysis of plane fretting fatigue (FF) contact problems are described, and new consequences for FF damage are derived. Constant normal load and oscillating tangential load (the celebrated Cattaneo–Mindlin case) are considered with in-phase oscillating moderate bulk stresses, for an arbitrary spline rotated geometry and, in particular, the flat punch with rounded corners in view of application to the dovetail joints.

Extremely simple, new results are found for initiation parameters such as tangential microslip and frictional energy, which have been used under certain conditions as threshold parameters for FF.

Finally, it is shown that for an "almost flat" geometry, the surface damage parameters decrease, but the tensile stress concentration increases, although it becomes more localized, suggesting that for cracks eventually initiated, the likelihood of self-arrest is higher than in the equivalent Hertzian case with same loads. This seems to interpret recent experiments, although it is not clear whether the optimal geometry in terms of FF life is the perfectly flat one, or an intermediate one.

Keywords: Contact stresses; Fretting fatigue; High cycle fatigue; Crack initiation; Fretting damage; Turbine blades; Dovetail joints; Gas turbine engines

1. Introduction

Fretting fatigue (FF) occurs when minute surface tangential motion arises between components pressed together by normal forces, and, if we refer to the data of the USAF (Thomson, 1998), is responsible for about one out of six in service 'mishaps' in gas turbine engines for which high cycle fatigue (HCF) is itself the largest single cause of failure. These two facts combine to give a clear idea of the relevance of the phenomenon for such safety-critical applications. Despite the remarkable progress, FF is still one of the

☆ An abstract of this paper was originally presented at the Sixth Pan American Congress of Applied Mechanics – PACAM VI, held in Rio de Janeiro, Brazil, 4–8 January 1999.

* Corresponding author.
E-mail address: m.ciavarella@area.ba.cnr.it (M. Ciavarella).

0020-7683/01/$ - see front matter
PII: S0020-7683(00)00136-0

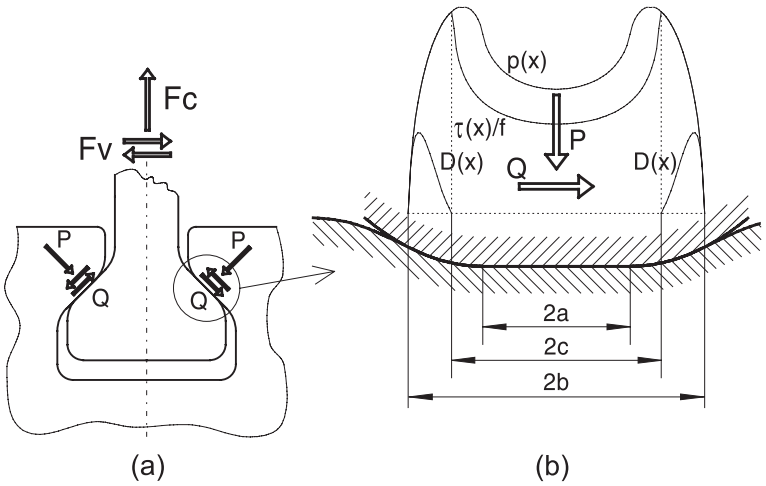

Fig. 1. Schematics of (a) dovetail joint geometry and (b) of the radiused flat contact model.

most "inexact" areas of fatigue, where effort is now being focused. In the USA, an attack has been launched with the Multi-University Research Initiative (MURI) program by the US Air Force, and many groups are now active on FF also in other parts of the world. Recent results appear in ASTM STP1367 (1999) and in a special issue of Int. J. Fatigue, vol. 21 (7), 1999.

The present paper is composed of four parts. In Section 1, after briefly reviewing some background material on historical developments of experimental and theoretical work on FF, models based on tangential microdisplacements, stress concentration, asperity contacts, and fracture mechanics, we conclude that, at present, the earliest models (microdisplacement and surface damage) are still valid for their simplicity and explanation of size effect because there is as yet no general agreement or definitive experimental evidence on alternative criteria, which are almost certainly more complex. Infact, microdisplacement and surface damage criteria are currently used as threshold factors of FF for qualitative ranking of materials (the ESDU database as given below) and also have physical interpretation in terms of asperity contact incremental strain models similar to the ones used with success in rolling contact fatigue. In Section 2, we review advances made, by the present authors, in analytical tools for the solution of plane partial slip contact problems, appropriate to fretting problems, for a general spline geometry (and in particular the dovetail joint geometry). In Section 3, we discuss the main part of the paper, extending results reviewed in Section 2 for the calculation of microdisplacement and surface damage. In Section 4, we finally focus on the dovetail joint geometry (Fig. 1a), reviewing results for pressure distribution, strength of the contact, stress intensity factors which were already presented only partly in earlier papers. The results for microdisplacement and surface damage for this geometry are completely new. In the discussion and conclusion section, we therefore try to infer some deduction for the FF behavior of dovetail joint, giving suggestions for design and further experiments.

2. Background

2.1. The early experiments and micro-displacement-based models

Early in the last century, fretting was identified in the specimen fractured in the grips of fatigue machines (Eden et al., 1911; Gillet and Mack, 1924), and tangential microdisplacements, δ_{max}, were suggested as

Table 1
The ESDU fatigue strength reduction factor K_{ff}, based on fretting microdisplacement (from Lindley, 1997)

K_{ff}	Low mean stress	High mean stress
$\delta < 0.005$	2	4
$\delta > 0.005$	2	10

quantifiers of the phenomenon (Tomlinson, 1927). More systematic investigations on FF in the 1940s recognized a small decrease of fatigue performance (13–17%) in previously fretted specimen (Warlow-Davis, 1941), but later on, it was pointed out that the *combined* effect of fretting and fatigue was much more severe causing a strength reduction of a factor 2–5 or more (McDowell, 1953). It was found that an FF limit seemed to be difficult to obtain even for materials with clear plain fatigue endurance limits.

In the 1960s, experiments on inert gas atmosphere showed that, although fretting wear decreased, the fretting strength was not significantly increased, confirming that the two processes have no direct relation. Nishioka et al. (1968) and Nishioka and Hirakawa (1969a,b,c) noticed a critical range of slip values promoting FF (δ_{max} of the order of 15 μm): not only at lower displacements, was there no significant fretting damage, but also at higher displacements because – it was suggested – wear eroding of the microcracks eventually initiated. Further studies, (Bramhall, 1973) found that, if only the dimension of the contact is changed and not the mean pressure and stress field, a critical size exists for the contact area dimension below which the FF life is much longer ($>10^7$) than above this limit. Similar experiments were conducted by Nowell (1988), confirming the presence of a "size effect".

It appears to be evident, therefore, that the microdisplacement-based model has dominated the scene and still is a very convenient and immediate 'rule of thumb' in orientating the engineer facing this complex phenomenon. In fact, the engineering sciences data unit (ESDU) in the UK has recently developed a practical fatigue strength reduction factor K_{ff} criterion from test data collected by the National Engineering Laboratory on carbon steel, based only on fretting microdisplacements and mean stress, as shown in Table 1.

This approach is remarkably simple, but should only be used for qualitative ranking of material combinations due to difficulties in applying results from simple specimen geometries to complex components (Lindley, 1997).

2.2. Attempts of more advanced fretting fatigue modeling

Few researchers have focused on stress concentration effects (Wright and O'Connor, 1972; Fenner et al., 1956). The difficulty of obtaining an accurate value for the elastic stress concentration factor K_t, for frictional contact problems, and the fact that the very steep gradients of the stress field and the other complex aspects of the phenomenon require a more complex modeling than the K_t-based approach, had probably demotivated the early researchers. Collins and Tovey (1972) suggested an 'asperity-contact microcrack' initiation mechanism based on fatigue stress concentration at the asperity level. Similar initiation models have also been attempted more recently (Ballard et al., 1995; Moobola, 1998). They are based on the idea that macroscopic stresses remain elastic, but microscopic stresses on the asperity level can locally exceed yield. In particular, the former (Ballard et al., 1995) proposes to examine the cyclic plastic response and predict initiation when the elastic shakedown limit is overpassed. However, for asperity-based approaches, as in general for rough contact theories, the fundamental question of the resolution at which measuring the "asperities-features" remains unsolved. Therefore, what one sees as asperity at one scale, develops into a complex pattern of asperities at the scale just below: the elastic solution predicts in the limit contact over an infinite set of points – a fractal set contact area (Ciavarella et al., 2000). This is clearly only a limiting condition but indicates that, as basically found by Archard (1957) already, the concepts of "pressure" and

"contact area" are not as obvious as one may think and depend very much on resolution of the measuring instrument. Every asperity has its stick-slip boundary (except from the ones in full slip), so the contact and the fortiori stick-slip boundaries are not as precisely defined as one may suppose from the classical macroscopic Cattaneo–Mindlin solution (Ciavarella et al., 1999).

Turning back to models for FF, an attempt was made by Ruiz et al. (1984, 1986) to combine the stress concentration/fretting damage approaches, with an empirical parameter taking account of tensile surface stresses also. FEM results and experiments on dovetail joints indicated a qualitative good prediction capability of the Ruiz parameter, but, as will be discussed in Section 3, the increased complexity of the Ruiz parameter does not necessarily corresponds to an increased predictive capability. Recently, other fatigue-based criteria have been proposed (Neu et al., 1999, which also contains a good review) but a general agreement has not been reached in modeling this complex phenomenon. Initiation models in the sense of fracture mechanics are discussed below.

2.3. The use of fracture mechanics and "crack analogue"

Another important attempt to model FF was fracture mechanics based, which probably started with Endo and Goto (1976): they recognized an initial propagation phase (faster than in plain fatigue) mainly due to shear with a small propagation depth inclined with respect to the surface and the principal stress. After this, there is a formation of a knee point where cracks turned and propagated perpendicularly to the surface. They also supposed that the surface fretting damage occurred in the first 20–25% of their life, ending with the turning at the knee point, after which only the stress field (combination of the decaying contact field and the more regular bulk stress field) was the propellant of the so-formed cracks. Fracture mechanics was also used by Edwards (1981), Hoeppner (1994) and Waterhouse (1981, p. 143–158). Some authors remark with pessimism that each FF case should be studied separately (Hoeppner and Gates, 1981). Work was very intense during the 1980s (Waterhouse, 1981, 1992; Nix and Lindley, 1985; Waterhouse and Lindley, 1993; Nowell, 1988; Hills and Nowell, 1994) and is becoming even more so recently, particularly due to extensive programs on fatigue such as the MURI program in the USA.

Due to difficulties in detecting a crack when it is not "too late", or designing for a crack to self-arrest (Moobola et al., 1998), it is not easy to use a "damage tolerant" design under HCF, so most of the effort is now concentrated on initiation (Fellows et al., 1997; Szolwinski et al., 1996; Fouvry et al., 1998; Nowell and Hills, 1990) or "short crack" models (Araujo and Nowell, 1999). Models are various, as initiation from fretting being more complex than initiation from a standard notch, the stress field being very severe and multiaxial, and also because shear tends to be very high promoting highly mixed-mode conditions. Giannakopoulos et al. (1998) consider the limiting case of a rigid sharp squared-end indentation, where the stress field induced by the contact is very similar to the square-root singular stress field around an external crack, proposing a *crack analogue* model. The exterior of the contact area is then like an infinite size crack; the singular stress field can be quantified by a stress intensity factor, and the bulk stress in the contacting materials becomes T – stress in the fracture mechanics terminology. Cracks developed at the contact site are kinked cracks, although the compressive stress field (which would cause contact of the equivalent crack faces) in mode I has no immediate correspondent in LEFM. Initiation can therefore be based on thresholds of stress intensity factor amplitudes $\Delta K < \Delta K_{\text{th}}$, typically at very high mixed-mode levels because the tangential load (perfect adhesion is assumed) is a mode II load and the torsion of the indenter is of a mode III nature. In practical cases, indenters are not rigid, the singularity is not the $-1/2$ singularity of the crack case, and partial slip arises rather than perfect adhesion. Of particular concern is the circumstance that, when the indenter is blunted as opposed to the case where a crack is blunted, the maximum stresses may localize the subsurface and as a result, the stresses are not only far from the singular limiting case but actually milder than a perfectly rounded indenter (Ciavarella, 1999). Nevertheless, the *crack analogue* model provides a length scale immediately to the problem (not the crack size, as it is virtually infinite, rather

the contact area size which is the size of the interior of the crack), and another explanation of the size effect found experimentally by Bramhall and Nowell.

3. Review of analytical results

3.1. Normal contact

Within the assumption of considering the bodies' elastically similar half-planes, the solution for the normal load can be obtained very simply as normal and shearing tractions are uncoupled: pure normal load does not induce shearing tractions, and any kind of tangential load does not alter the pressure distribution. General solutions have been known for some time, and detailed solutions have been obtained for the pressure distribution induced in a generic quadratic spline profile contact (Ciavarella and Demelio, 1999), dealing with the general case of non-symmetrical indentation, where the position as well as the dimension of the contact area vary with load. This solution covers all cases of engineering interest as long as the contact area is connected. First, the geometry of the problem is entirely defined by the function $h(x)$

$$h(x) = T_y + \alpha x - [f_1(x) - f_2(x)], \tag{3.1}$$

where $f_1(x)$, $f_2(x)$ describe the bodies' profiles, and T_y, α are the normal and rotational components, respectively, of the rigid body motion that brings the two bodies into contact. The normal traction distribution over the contact is given by the following integral equation (Hills et al., 1993, f. 2.17 p. 51), over the unknown contact region L

$$\frac{1}{A}h'(x) = \frac{1}{\pi}\int_L \frac{p(\xi)\mathrm{d}\xi}{x-\xi}. \tag{3.2}$$

Here, A is the "composite compliance" of the bodies, which in plane strain is (E_i is Young's modulus and v_i is Poisson's ratio of body i)

$$A = \frac{2}{E_1}\left(1-v_1^2\right) + \frac{2}{E_2}\left(1-v_2^2\right). \tag{3.3}$$

In Ciavarella and Demelio (1999), a detailed solution for a generic quadratic spline profile, allowing unsymmetrical indenter geometries, and therefore, implicitly, for the influence of tilt, has been given. The overlap function $h_0'(x) = h'(x) - \alpha$ is given as a spline composed of n parabolic functions, i.e. in the ith interval ($i = 1, \ldots, n$), by

$$h_0'(x) = m_i x + D_i, \quad x_i < x < x_{i+1}. \tag{3.4}$$

The solution for the pressure distribution, load and resulting moment is given in Ciavarella and Demelio (1999).

3.2. Partial slip

Solutions for normal load other than Hertzian geometry have been known for some time, and the range of solutions for frictional problems causing partial slip which were essential to study fretting in detail was much more restricted. The classical solution was that relating to a tangential load applied sequentially to a Hertzian contact, originally devised by Cattaneo (1938), and independently by Mindlin (1949) after Cattaneo (1947a,b) had also solved the case when the contacting bodies were described by fourth-order surfaces. Further progress was made on more general loading history for the Hertzian geometry by Mindlin

and coworkers, or on the limited effect caused by elastic dissimilarity – for a review, see Hills and Sosa (1999).

A more general solution to the Cattaneo–Mindlin problem for any plane contact problem (not necessarily Hertzian) was given in Ciavarella (1998a,b) proving that the Cattaneo frictional traction distribution

$$q(x) = f[p(x) - q^*(x)] \tag{3.5}$$

satisfies both equality and inequality conditions, with $q^*(x)$ being the normal contact pressure distribution at some smaller value of the normal load. Upon increasing the tangential force, the stick zone shrinks in the reverse order as the normal contact area during the normal loading process. The more general loading scenarios where normal load is not held constant (Mindlin problem) has been treated by Jaeger (1998). General three-dimensional geometry also permits this solution strictly only for the case where Poisson's ratio is zero (Ciavarella, 1998c) and only where the sign, but not the direction of the tangential force, changes. Otherwise, there is a mismatch between the direction of the traction and the direction of slip, indicating that both components of shearing tractions are needed for the correct solution. However, this is also true for the original Cattaneo–Mindlin solutions, and error has been shown to be small in particular cases.

The application of these results to fretting contact problems was shown in Ciavarella et al. (1999a), and further extension to the case of 'moderate' bulk strain present in one of the contacting bodies, and oscillating in phase with the tangential loading, was shown in Ciavarella et al. (1999b). Further interesting corollaries were shown in Ciavarella and Hills (1999), namely that the effect of wear which eventually alters the geometry in the region of the microslip will not change the dimension and location of the region of stick with the result that in principle, the pressure will localize within these region, and in the limit, a singularity of pressure would arise at the slip-stick transition point. The most general case of loading condition may require a numerical scheme, and an efficient one makes use of Kalker's optimization theorems, as discussed in detail in Dai and Nowell (1998). Techniques for the internal stress and displacement field calculations are then routine either based on a series solution for Muskelishvili's potential or as a piecewise linear discretized form of the pressure using overlapping triangles (Kelly et al., 1997).

In any real application, specifically in a dovetail joint of a typical gas turbine engine, there are components of load that are varying with the regime like centrifugal loads, others that vary with power output (fluid pressure), and others that are induced by vibrations. Also, even if only one of these loading effects is considered at a time, typically not only one component of load in the contact is affected because of offsets and asymmetry of the contact: in other words, an increase in centrifugal loads induces an increase in both normal and tangential load as well as an offset of such loads with respect to the original direction. Studying such conditions require a very detailed analysis of the general Mindlin problem case, and although this is in principle possible (Jaeger, 1998), we limit our interest here to the case of constant normal load P and oscillating tangential load Q.

In particular, we consider, as in Ciavarella et al. (1999b), a surface tension which develops simultaneously and in proportion to Q. Provided that the surface strain is only *moderate*, we can, in fact, assume that slip zones of the same sign occur, and the general solution is given by Eq. (3.5), where the corrective pressure, $q^*(x)$, is the solution of the following integral equation:

$$\frac{1}{\pi}\int_{S_{\text{stick}}} \frac{q^*(\xi)}{x-\xi}\mathrm{d}\xi = \frac{1}{A}h^{*\prime}(x), \quad x \in S_{\text{stick}}, \tag{3.6}$$

which can be recognized as being of the same *form* as the original equation for normal contact, Eq. (3.2), with a lower normal load, Q^*, and a modified right-hand side with

$$h^{*\prime}(x) = h'(x) - e_x = \left(\alpha - \frac{e_x}{f}\right) - \left[f_1'(x) - f_2'(x)\right]. \tag{3.7}$$

Thus, we can define a fictitious rotation, $\alpha^* = (\alpha - e_x/f)$, i.e. the *geometrical* rotation reduced by e_x/f. The condition for this 'corrective' solution to hold is that the stick zone has to be contained entirely within the contact area. If it lies partly outside, this means that the initial assumption of moderate surface strain is violated, and the solution needs, in general, a numerical procedure. The case of oscillatory loading can be easily covered by generalizing the above argument with a series of superposition of normal contacts, and indeed it may be important to consider frictional residual stresses to find the highest stress ranges on each loading phase. The details of the partial slip solution for the geometries under examination have been presented elsewhere (Ciavarella et al., 1998). A more complete analysis, where the indentation is not symmetric and bulk strains are also present is reported in Ciavarella et al. (1999b).

4. Application to fretting damage parameters

As seen in Section 2, experimental evidence indicates that the detrimental effect of fretting occurs only in certain ranges of conditions. The complexity of the phenomenon and the relatively reduced number of tests available, with respect to plain fatigue, have complicated the separation of the different effects which are believed to influence the phenomenon. It may be said that FF moves at the boundary between conditions which are more deeply understood and may serve as bounds for orientating the analysis. These are, in short (i) rolling contact fatigue, (ii) fatigue crack initiation and propagation from a notch, and (iii) fatigue crack initiation and propagation as directly applied to the "crack analogue".

The former (i), which has been quite successfully attacked in the context of ball bearings design, starts from the consideration that unidirectional passes of a moving (rolling, sliding) contact load causes sub-surface in a strain hardening material and incremental plastic shear strain (Bower and Johnson, 1989). In fretting, the motion is not unidirectional, but hysteresis cycle of the frictional surface tractions causes at asperity level, the possibility of incremental plastic shear strain; this justifies the choice of classical damage parameters.

(1) Slip amplitude $\delta_{\max}$, where δ is the relative tangential displacement of contacting particles during the cycle, proportional, for a pair of surfaces of a given roughness, to the number of asperity passes per cycle (Nowell and Hills, 1990).

(2) Frictional energy dissipation parameter $D_{\max} = (\tau\delta)_{\max}$, also called F_1 or fretting wear parameter, which gives a measure of the cumulated strain according to Bower–Johnson's mechanism. In fact, $\tau = fp$ in the slip regions, and p from classical rough contact models like that of Greenwood–Williamson is in turn proportional to the number of asperity contacts per unit surface (Kuno et al., 1989, and see a detailed discussion in Section 5 of Nowell and Hills, 1990). Finally, D may also be interpreted as the surface energy expenditure per unit surface area.

However, in fretting, the coefficient of friction is typically much higher than in ball bearings (and it increases even more during the fretting cycles, so that it is not uncommon to find values higher than 0.75), and therefore, the mechanisms may differ as maximum shear occurs at the surface. Also, the higher friction coefficient means that tensile stress concentration is much higher, activating mechanisms (ii) and (iii). There are no systematic studies correlating the elastic stress concentration factor, K_t, on FF life, except recent ones (Szolwinski and Farris, 1998), which propose a more refined criterion based on the Smith–Watson–Topper equation. They introduce an 'experimental' nucleation life as the difference between the observed failure life and the 'estimated propagation life' which is defined as the time needed to propagate a certain length of crack from a certain starting dimension. This criterion may also explain the size effect as in the 'estimated propagation life', there is a length scale, but the authors indicate that this 'estimated propagation life' is only 10–15% of the total life, and therefore cannot take account of any significant size effect as found by Nowell and Hills (1990). Indeed, there is no clear indication that the estimated propagation life of the

Nowell and Hills (1990) paper has been quantified in that paper (Szolwinski and Farris, 1998), so that the two facts combine to render obscure the reason why the experiments seem to fit, unless only a subset of the Nowell and Hills (1990) data has been used.

It is clear that a correct fatigue approach needs a fatigue stress concentration factor (SCF) K_f, rather than the purely elastic SCF, K_t. K_f is defined as the ratio between degradation from the ideal plain fatigue limit to the actual limit and obviously $K_f < K_t$. The fact that the tensile concentration is very localized in contact indicates that the actual K_f is probably very far from K_t. Notice, however, that this may be a further alternative explanation of the size effect noticed by Bramhall and Nowell studies: indeed, a first estimate of K_f may be obtained using a "hot spot approach", i.e. considering the stress concentration at a certain, material dependent distance from the stress raiser. For example, Taylor (1999) propose to consider a point at a distance $a_0/2$ from the actual stress maximum, where a_0 is an intrinsic size of the material which depend on fatigue limit $\Delta\sigma_1$ and threshold ΔK_{th} by considering that $\Delta K_{th} = \Delta\sigma_1\sqrt{\pi a_0}$. It is clear that the maximum size effect possible is the one given by considering a $1/2$ singularity, i.e. considering the contact area as a crack (the "crack analogue" model), and further analysis of the size effect may lead to a better understanding of the phenomenon.

Another damage parameter used in an attempt to consider tensile stresses is

(3) $R_{max} = (\sigma\tau\delta)_{max}$, also called F_2 or FF parameter, introduced by Ruiz et al. (1984), which empirically takes into account the evidence that cracks are more likely to develop in regions of tension rather than compression, therefore accounting also for the early stages of propagation. It has some success in predicting the likely initiation sites, but there is no reason to believe it may work for quantitative analysis. In fact, R, although apparently more "comprehensive", has no direct physical interpretation, and, more importantly, is a hybrid approach which measures two competing processes by multiplying them arbitrarily with the same weight and at the same point.

Recent experiments (Iyer and Mall, 1999) found a decrease in FF life with increasing normal loads, whereas all three parameters, δ_{max}, D_{max}, R_{max} would predict an increase. Vice versa, the experiments correlated well with the local maxima of stress ranges (which, due to frictional residual stresses, is much larger than what expected). However, this criterion would not work in the Bramhall (1973) and Nowell (1988) kind of experiments, mentioned above, where only the size changes so that any chosen stress range would remain constant, whereas FF life decreases sharply when the contact size exceeds a certain threshold. A tentative hypothesis we may put forward is that any of δ_{max}, D_{max}, R_{max} may be used as threshold parameters as there is no evidence that they can be used as a continuous indicator of FF life.

The fact that R depends strongly on the surface stress σ, which in turn is the sum of three separate contributions [1] giving a subsequent dependence on several other parameters, renders it very difficult to show comprehensive results. Hence, results for R would need a separate investigation, but will not necessarily provide really definitive answers. Attention will be focused here on the first two, slip amplitude, δ_{max}, and frictional energy parameter, D, only and in particular, we will examine its distribution for the flat indenter, with radiused edges, and compare it with the classical Hertzian case. Comparisons and new results will be displayed, permitting a better insight into the phenomenon of fretting damage in real contacts.

4.1. Tangential microdisplacements

The displacements within the slip region are found from the general solution of the partial slip problem. The full sliding component can, in general, be integrated directly from an expression given in terms of the

[1] The surface stress is given by the bulk stress, the stress induced by the tangential contact tractions, proportional to the friction coefficient, and the additional stress due to finite thickness of the contacting bodies (Fellows et al., 1995).

geometry, whereas the corrective term depends on q^*. Further, considering that the relative tangential displacements are zero in the stick region, and at any particular point x_0 inside the stick region, we obtain

$$u_x(x) = f[h(x) - h(x_0)] - \frac{fA}{\pi}\int_{x_0}^{x}\int_{L_{\text{stick}}}\frac{q^*(\xi)\mathrm{d}\xi}{x-\xi}\mathrm{d}x, \quad x \in L_{\text{slip}}. \tag{4.1}$$

By reversing the order of integration and performing the integral, we find

$$u_x(x) = f[h(x) - h(x_0)] - \frac{fA}{\pi}\int_{L_{\text{stick}}} q^*(\xi)\ln\left|\frac{x-\xi}{x_0-\xi}\right|\mathrm{d}\xi, \quad x \in L_{\text{slip}}, \tag{4.2}$$

where we have defined a gap function, $g(x) = [h(x) - h(x_0)]$. A complete description of the surface displacement may be found straightforwardly. A very simple result can then be obtained in the limiting full sliding conditions, i.e. under incipient full sliding:

$$u_x(x) = fg(x), \quad x \in L, \tag{4.3}$$

a result of immediate graphical visualization, which provides the upper bound for the displacement before the full slip condition, above which they become indeterminate.

4.2. Frictional damage D

From the definition of D, we see that

$$D(x) = u_x(x)\tau(x) = u_x(x)fp(x), \quad x \in L_{\text{slip}}$$

and the components of this product are now known. In particular, the limiting value is easily seen from the initial gap function. Under such conditions, we have from (4.3)

$$D_{\text{lim}} = u_x(x)fp(x) = f^2 g(x)p(x) \tag{4.4}$$

from which it is clear that the two components of damage have opposing effects: where the gap is higher, the pressure (and hence the shear traction) will tend to be lower, and vice versa, so that the damage parameter tends to be a weak function of geometry, as it will be found below.

If we consider the integral of the local parameter D over the contact area, we obtain a measure of the energy expended at the contact in the fretting regime, i.e.

$$E = \int_{L_{\text{slip}}} D(x)\mathrm{d}x. \tag{4.5}$$

5. The rounded flat geometry – dovetail joints

Here, we collect results for the case of interest for the design of dovetail joints, i.e. for rounded flat indentation, which we assume to be symmetrical in geometry and loading conditions for simplicity, some remarks on the more general case being in Ciavarella and Demelio (1999). We then add the original results for the section relative to damage parameters.

Until recently, mostly Hertzian contacts were used for quantitative FF testing because the interpretation of the stress field was only available in closed form (Hills and Nowell, 1992, 1994). However, the Hertzian geometry is very remote from those found in engineering applications such as splines and dovetail joints for blades of gas-turbine engines. If the contact conditions are to resemble real dovetail joint contacts (Fig. 1a), flat indenters with rounded corners (Fig. 1b) present a most interesting choice, and indeed, the contact pressure distribution they develop is very close to real applications to both dovetails joints and spline

couplings. The use of indenters having this form has several advantages over the alternatives; testing using Hertzian indenters means that, whilst the contact pressure and shearing traction may be adjusted to take prototypical values, the surface slip displacement, being proportional to the integral of the stress field, will not, and this lack of fidelity in the test geometry may have consequences for the interpretation of the fatigue results found. As both the stress field and the displacement field of the prototype are replicated faithfully, the so-called "size effect" may be explored, i.e. the different FF behavior of materials under geometrically identical contacts of varying size. Several authors are now performing experiments with this geometry, including Hutson et al. (1999), and Pape and Neu (1999). In particular, Pape and Neu (1999) use, simultaneously under same nominal contact load, a flat-on-flat and a cylinder-on-flat contact configurations on opposite sides of a FF specimen; the major fatigue crack always occurred at a cylinder-on-flat contact. Similarly, Hutson et al. (1999) noticed an increase of the fretting life for smaller radii in the rounded flat specimen, an occurrence which is quite surprising from a classical fatigue point of view. This suggests that the fact that there is virtually no microslip for the perfectly flat contact may be the theoretical optimal condition for FF, which would be quite surprising. Alternatively, there may be an "almost flat geometry", perhaps depending on materials and loading conditions, to give the best FF performances. In an attempt to interpret these results, we give results for pressure distribution, strength of the contact, partial slip, damage parameters, and stress intensity factors.

5.1. Contact laws

We have seen above that a general solution to the spline profile has been obtained in Ciavarella et al. (1998). However, particular results which are of immediate interest here are (i) the case of a Hertzian, *parabolic* indenter with $k = 1/R$, the local curvature at the point of first contact, for which the following well-known results are obtained:

$$\frac{AP}{k} = \frac{\pi}{2} b^2, \tag{5.1}$$

$$\frac{b}{P} p(\varphi) = -\frac{2}{\pi} \cos\varphi = -\frac{2}{\pi} \sqrt{1 - \left(\frac{x}{b}\right)^2}, \tag{5.2}$$

where $x = b \sin\varphi$, b being the contact half-width; and (ii) the case of a *flat punch with rounded corners*, where the same notation is employed and with a contact half length $b(= a/\sin\varphi_0)$

$$\frac{bp(\varphi)}{P} = -\frac{2/\pi}{\pi - 2\varphi_0 - \sin 2\varphi_0} \left[(\pi - 2\varphi_0)\cos\varphi + \ln\left(\left| \frac{\sin(\varphi + \varphi_0)}{\sin(\varphi - \varphi_0)} \right|^{\sin\varphi} \left| \tan\frac{\varphi + \varphi_0}{2} \tan\frac{\varphi - \varphi_0}{2} \right|^{\sin\varphi_0} \right) \right]. \tag{5.3}$$

With this implicit form of the pressure distribution, the contact law is more complex to find, but, considering a as a known geometrical quantity, the angle φ_0, and so the contact area as a function of the load P is found from equilibrium considerations to be

$$\frac{PAR}{a^2} = \frac{\pi - 2\varphi_0}{2\sin^2\varphi_0} - \cot\varphi_0, \tag{5.4}$$

where R is the edge radius. Eq. (5.3) then gives the pressure in the region $-\pi/2 < \varphi < \pi/2$, which corresponds to $-b < x < b$. It is interesting to note that the non-dimensionalized pressure does not depend

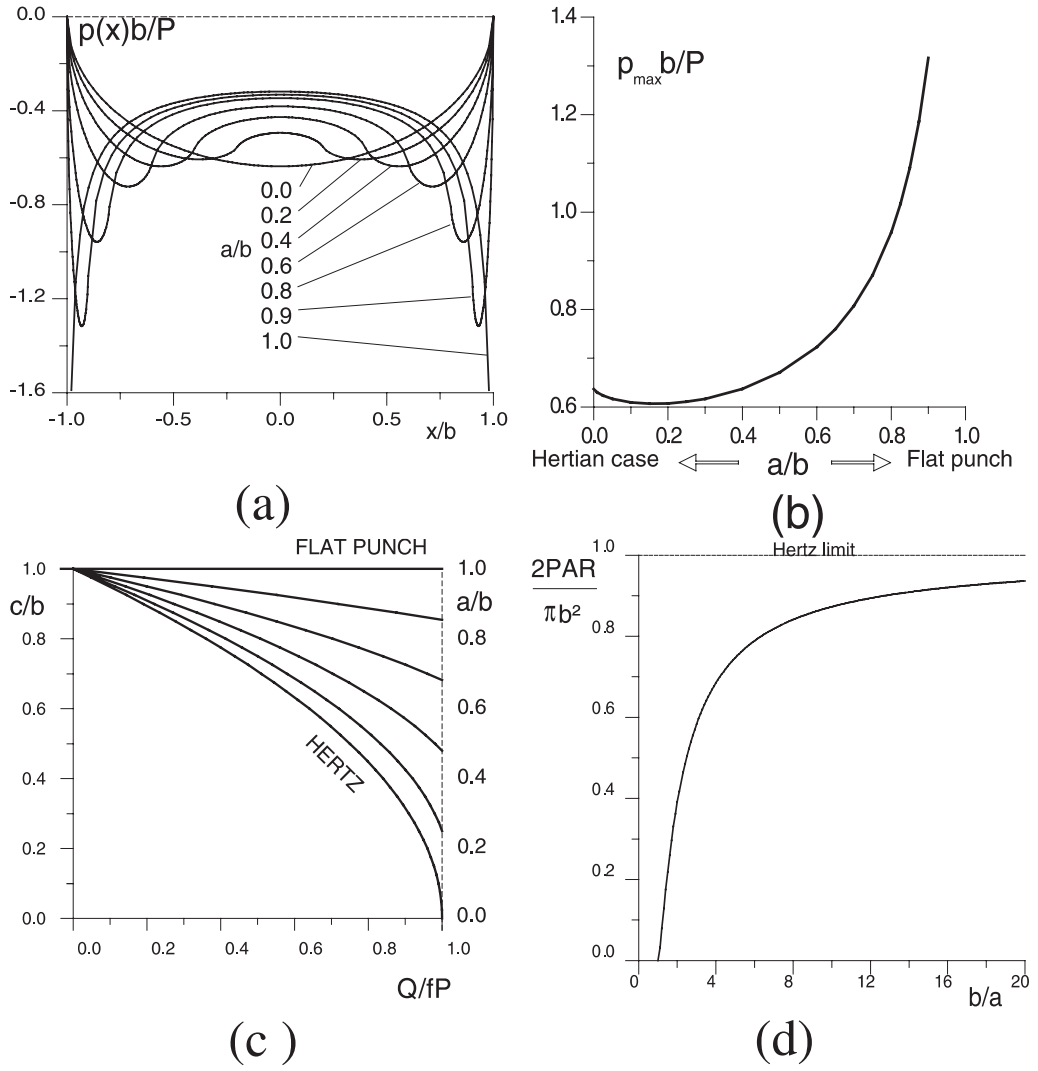

Fig. 2. The contact problem for the radiused flat contact geometry (symmetrical contact): (a) pressure distribution, (b) maximum pressure, (c) the stick area size c/b vs. tangential load ratio Q/fP, and (d) load parameter $2PAR/(\pi b^2)$ vs. contact area size b/a.

directly on R: in fact, for a given ratio b/a, only the absolute load will vary with R, according to Eq. (5.4). Fig. 2a gives the pressure distribution for contacts of this type ranging from the Hertzian indenter ($a/b \to 0$) to a quite sharp one ($a/b \to 0.9$). Notice that any rounded flat indenter for light loads, will have a low a/b, whereas for higher loads, the ratio a/b will become increasingly small (Hertzian). For comparison purposes, we have also represented the solution for a perfectly sharp rigid indenter, indicated as $a/b = 1$. Fig. 2b gives the maximum value of the pressure, where it can be observed that the peak pressure is higher than in the Hertzian case only for very small edge radii. The partial slip solution gives a dimension of stick area vs. loading ratio given in Fig. 2c. Notice that the higher a/b, the smaller the microslip region. Finally, Fig. 2d shows the loading parameter $2PAR/\pi b^2$ against the contact area ratio b/a, which may permit a graphical solution of the non-linear load Eq. (5.4).

More importantly for metals, it is the maximum value of the Von Mises parameter that is relevant for avoiding yield, and for purely normal loading conditions, the trend is similar to that obtained for the maximum pressure (although the maximum Mises value occurs at the subsurface, and it is not directly linked to the maximum of the pressure), and precisely, the strength is higher than in the Hertzian case in the range $a/b = 0$–0.5 (for additional details, see Ciavarella et al. (1998)). However, for ratios a/b higher than 0.5, the decrease in strength is quite rapid, and at $a/b = 0.9$, the strength is already halved with respect to the Hertzian case, which suggests that this limit is better not overpassed. In the fretting case, we need to consider the additional stress induced by shear tractions, for which a complete set of results for the partial slip case and different Poisson's ratios would be impractical to display here. Nevertheless, in the full sliding limit, we can plot results as in Fig. 3a–c for different Poisson's ratios ((a) $\nu = 0$ or plane stress, (b) $\nu = 0.25$ plane strain, (c) $\nu = 0.5$ plane strain). The point where the curves change curvature is the "subsurface-to-surface point" with the passage from subsurface-to-surface maxima. The higher the friction coefficient, the smaller the interval of a/b over which the strength is higher than the Hertzian value, until after the subsurface-to-surface point around $f > 0.3$, the highest strength is again the Hertzian. Notice also that in plane stress, there is no subsurface maxima. Also of some interest would be the exact location of the maxima, in order to understand the interaction with the tensile stress maxima which are always on surface. In fact, for low friction coefficient, the tension is small (normal load does not induce any tension) and the shear mechanisms subsurface prevail, as studied in rolling bearings fatigue; for higher friction coefficient, the two mechanisms interact. When the Mises maximum is on the surface, it is always at the trailing edge of the contact, whereas when it is in the subsurface, it depends on the ratio a/b. In fact, in the Hertzian case, it

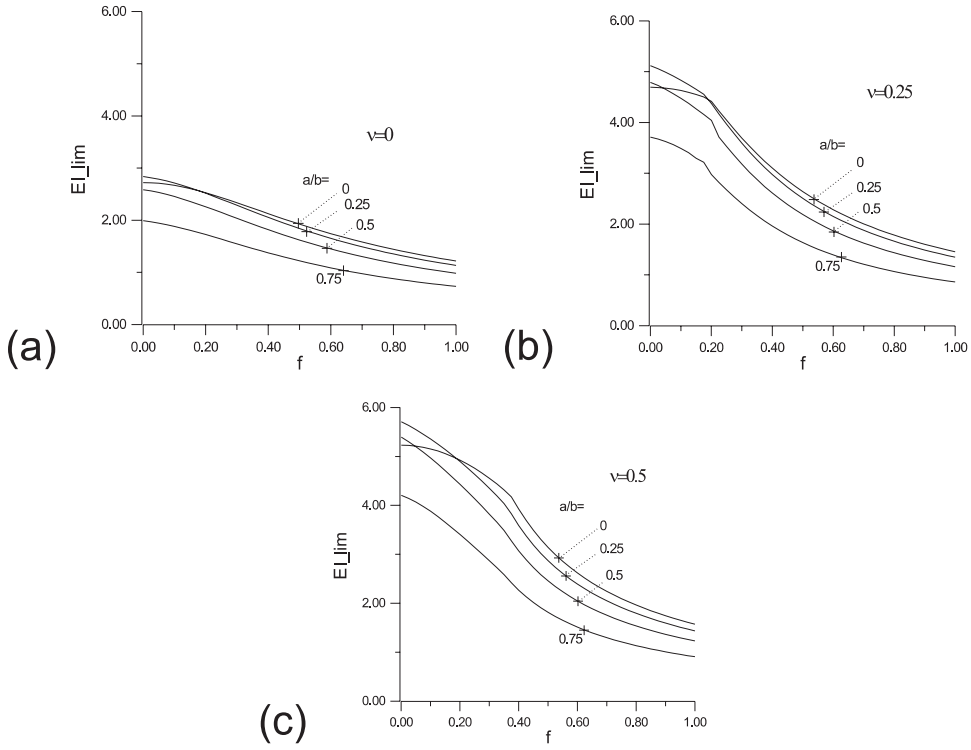

Fig. 3. Elastic limit $\mathrm{El}_{\mathrm{lim}} = P/bk$, where k is the yield stress under shear, in the case of full sliding, as a function of friction coefficient f. (a) $\nu = 0$ (or plane stress), (b) $\nu = 0.25$, and (c) $\nu = 0.5$ (incompressible material).

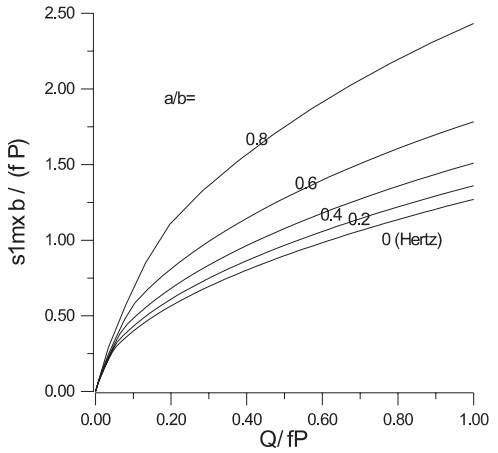

Fig. 4. Highest value of tensile principal stress in partial slip, $s1_{\max}b/(fP)$, as a function of loading ratio Q/fP.

moves from the centerline of purely normal load towards the surface, whereas in the rounded flat case, there are two maxima in the purely normal load case, symmetric with respect to the centerline, and closer to the surface a/b is higher.

The tensile stress maxima (we refer here obviously only to the contact-induced stresses) are more easily displayed in Fig. 4, as they are always localized at the trailing edge of the contact, they are only dependent of the shear traction (and consequently depend linearly on friction coefficient) always on the surface. Notice that they increase without limit when the ratio a/b is increased towards the flat indenter case.

5.2. Damage parameters

In the case of Hertzian geometry, the relative tangential displacements outside the stick region (x is normalized with respect to c), relative to the stuck point $x = 1$, are

$$2Ru_x(x)/\left(fc^2\right) = x\sqrt{x^2-1} - \log\left(x+\sqrt{x^2-1}\right), \quad x > 1 \tag{5.5}$$

or, using the Hertzian formula for the contact law

$$\begin{aligned} u_x(x) &= f\left(\frac{c}{b}\right)^2 \frac{b^2}{2R}\left[x\sqrt{x^2-1} - \log\left(x+\sqrt{x^2-1}\right)\right] \\ &= 2f\left(\frac{c}{b}\right)^2 \frac{A}{\pi} p_m b\left[x\sqrt{x^2-1} - \log\left(x+\sqrt{x^2-1}\right)\right]. \end{aligned} \tag{5.6}$$

The energy damage is therefore

$$D = D_0\left(\frac{c}{b}\right)^2\left[x\sqrt{x^2-1} - \log\left(x+\sqrt{x^2-1}\right)\right]\sqrt{1-x^2\left(\frac{c}{b}\right)^2}, \tag{5.7}$$

where we have introduced the normalizing factor:

$$D_0 = \frac{8}{\pi}(fp_m)^2\frac{A}{\pi}b, \tag{5.8}$$

which give an immediate evidence of the fact that friction coefficient and average pressure are the most important parameters affecting the fretting damage. The question of lubricating the joint is clearly very

interesting, and indeed there are recent studies on this factor – in particular, solid lubricant is most efficient in the partial slip regime while grease and oil, particularly the latter, are more suitable in the gross slip regime (Zhou and Vincent, 1999).

Turning back to the damage parameter in the limit case of incipient full sliding, we have for the Hertzian case,

$$D_{\lim} = f^2 \frac{x^2}{2R} \frac{4}{\pi} p_m \sqrt{1 - \left(\frac{x}{b}\right)^2}, \tag{5.9}$$

whereas for the rounded flat indenter case, the limiting value in the rounded part region is

$$D_{\lim} = f^2 \frac{(x-a)^2}{2R} p(x), \tag{5.10}$$

where $p(x)$ is given in Eq. (5.3).

Fig. 5 shows a representative case of tangential displacements, shear tractions and non-dimensional damage, for the case $a/b = 0.5$. Notice that the non-dimensional factors permit to use the same scale. If we move to consider only the limiting case (i.e. in incipient full sliding), we obtain Fig. 6, where for different geometrical ratio a/b, we notice a localization of the surface damage, but a surprisingly less marked decrease of the maximum value. Indeed, as shown in Fig. 7, the maximum value of the limiting damage parameter does not tend to zero as one would expect, and is only "weakly" dependent on geometry. Vice versa, the total energy obviously tends to zero – as expected from the partial slip behavior, the flat punch allows an oscillating tangential load (below the full sliding limit $Q/fP = 1$) without any frictional dissipation.

Given these maximum values, the dependence on Q/fP permits one to have a complete picture, and this is shown in Fig. 8 for both microdisplacements and frictional damage. In the log–log plot, these curves are almost linear, permitting a practical approximation for manual calculations.

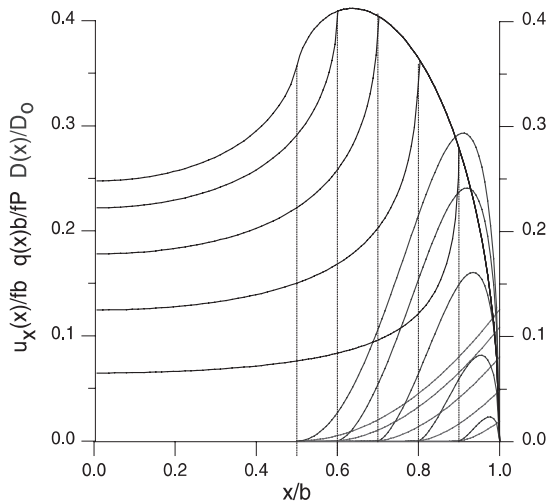

Fig. 5. Shear tractions, tangential microdisplacements and frictional damage D in partial slip, for an indenter with $a/b = 0.5$. The different cases correspond to different sizes of stick region, i.e. $c/b = 0.5$ (incipient full sliding), $c/b = 0.6$, 0.7, 0.8, 0.9.

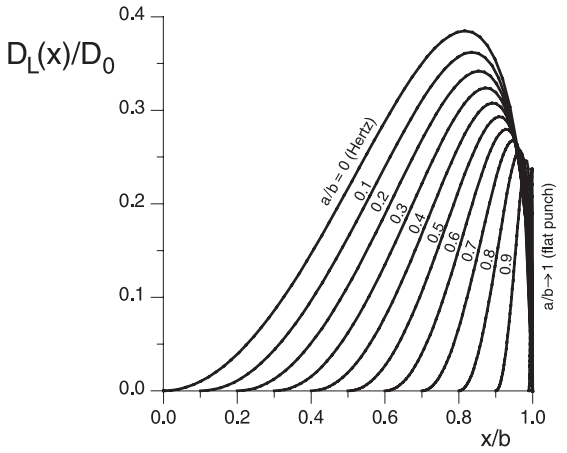

Fig. 6. Limiting value of frictional damage D in incipient full sliding, for different geometrical ratios $a/b = 0$ (Hz), $0.1, \ldots, 0.9,\ 0.999$ (flat punch).

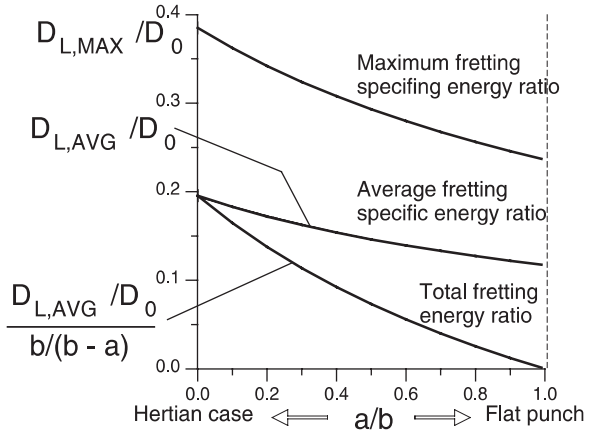

Fig. 7. Maximum and average values of the limiting frictional damage D_L and of the total frictional energy in incipient full sliding as a function of the geometrical ratio a/b.

5.3. Stress intensity factors

In previous papers (Ciavarella et al., 1999a), we have already approached the calculation of stress intensity factors for cracks developing from the surface of the fretted specimen having a rounded flat indenter geometry. However, the range of results is, in theory, very large as there are many independent variables. Therefore, here we present a more complete set.

It is clear that these quantities may be found reliably, if the crack dimension is large enough, compared to the average grain size of the material. It is not within the scope of the present paper to give a detailed presentation of the well established semi-analytical techniques using distributed dislocations for the solution of the crack problem, but we only recollect that the basic assumption is that the presence of the crack does not influence the contact tractions, and the validity of this assumption has been demonstrated in previous experiences with related problems (Munisamy et al., 1995). The crack problem can then be solved

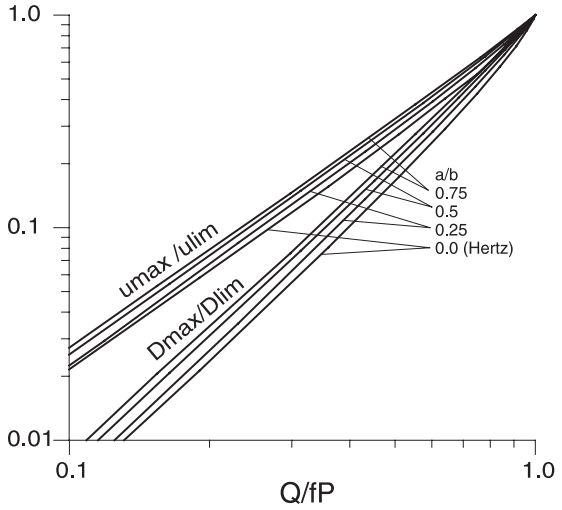

Fig. 8. Maximum values of microdisplacements and frictional damage D with respect to the limiting ones in incipient full sliding as a function of the loading ratio Q/fP.

by distributing dislocation in the half-plane, and the stress state induced by the resulting distribution gives an integral equation, the right-hand side of which is given by the tractions along the line of the crack but in its absence, which we can find with the techniques described above (for more details, see Hills et al., 1996). The solution is then numerical routine, and the stress intensity factors are found from the dislocation density at the crack tip.

For a crack initiated at the contact trailing edge, the overall stress state experienced by the crack tip, particularly during the early stages, is significantly influenced by the contact stress field, so that there is a period when the crack is almost invariably growing into a decreasing stress field. The analogous set of circumstances in plain fatigue is when a crack initiates at a notch. In either case, it is possible that the decrease in crack tip stress intensity factor may be so great that self-arrest occurs, and a relatively benign defect remains which will suffer no further growth. Evidence of this is seen in the wedge bars found in electrical generators, and the swashplates units fitted in helicopter rotor heads. It may be remarked that this phenomenon provides the possibility of one approach towards a safe (infinite life) design; the stress intensity factor history for a developing crack may be estimated, and the minimum value found. If this is below the threshold stress intensity factor (or, more conservatively, becomes negative), arrest is certain. Calculations following these lines have been carried out for the Hertzian geometry (Moobola et al., 1998) for which it has been found that this is a practical approach only in cases where the bulk loading (which in turbine blades dovetail joints is the significant centrifugal stress) is relatively moderate, and serious surface shearing tractions are present: in other cases, it is almost invariably found that the crack tip stress intensity increases monotonically with crack length. As we will see below, the rounded flat geometry shows a larger range of self-arrest conditions.

In Ciavarella et al. (1999a), some results for stress intensity factors have already been shown. Here, we obtain a larger set for friction coefficient $f = 0.2, 0.4$, a bulk stress $s_{\text{bulk}} = \sigma b/P = 0.1, 0.2$, $Q/fP = 0.3, 0.9$. The results are shown in Fig. 9. Specifically, they give the mode I stress intensity factor, $K_{1n} = bK_1/(P\sqrt{\pi b})$ for the given set of parameters. Notice that here the bulk load was considered constant in time, so that the stick region would not be affected. The results clearly are only representative of various possible conditions, are not considering the details of the crack initiation inclined to the surface, and do not consider details of non-symmetrical shear traction distribution. However, they indicate clearly that for higher a/b ratio,

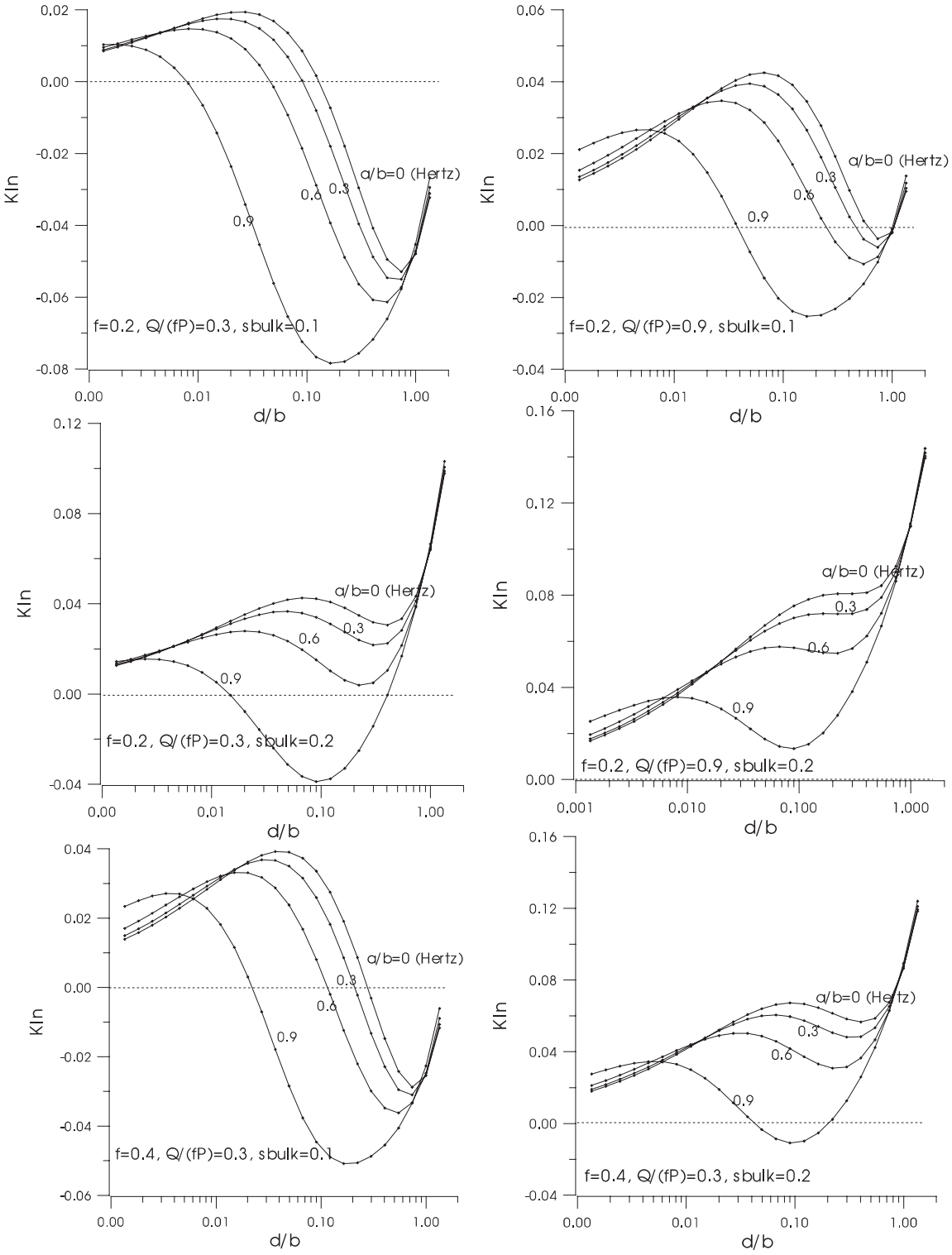

Fig. 9. Non-dimensional mode I stress intensity factors $K_{In} = bK_I/[P\sqrt{(\pi b)}]$.

although as seen in Fig. 8, the tensile stress is initially larger at the surface, it becomes also much more localized. Therefore, for high a/b ratios, we obtain rapidly a decrease of the SIF, which may easily cause self-arrest. Notice, also that the effect of doubling f is not as significant as doubling the bulk stress.

In the early stages of propagation, namely $d/b < 0.4$, the effect of geometry on K_I appears to be very significant: in the limiting flat punch case ($a/b = 1$) K_I starts practically from minus infinity and is highly negative until a very large size of the crack is reached ($d/b = 1.2$) for the specific case; on the contrary, for a Hertzian pad ($a/b = 0$), the crack is open from the earliest stages, but can possibly reach conditions of self-arrest, as it has been studied for a complete set of loading conditions in Moobola et al. (1998). An equally complete set of results for the flat punch and all intermediate geometry is not available at present, but it is clear from the results of Fig. 4a that self-arrest is much more likely to occur in this case rather than in the Hertzian one, which represent an upper bound to all curves of the rounded flat indenters. Specifically, self-arrest in the Hertzian case could occur anywhere in the range $0.4 < d/b < 1.2$, whereas for an almost flat geometry, at $a/b = 0.75$, self-arrest occurs anywhere in the range $0.15 < d/b < 1.2$.

In most cases, as the crack reaches a length equal to about 70–80% of the contact half-length, the effect of geometry is practically negligible, with the outcome that the stress intensity factors are a function only of the resultant load; although a similar result was to be expected from an application of St. Venant's principle, it was not obvious from the outset that this would happen at such modest distances from the contact itself.

The analysis does not consider the possible influence of K_{II}, and of the resulting initially inclined crack, but they permit nevertheless to figure a strong indication that the use of an almost flat pad with the proposed geometry resists FF crack propagation.

6. Conclusions

Analytical methods for the study of typical fretting partial slip contact problems in turbine engines dovetail joints have been reviewed. Arbitrarily complex spline geometries can be used for modeling cases of interest as long as the hypothesis of approximating the contacting bodies as half-planes is maintained, and the influence of very complex loading cycles conditions can be neglected. Similar precise analyses were previously limited to the simplest Hertzian contacts. The implications on fretting damage parameters of common use, such as microdisplacements and frictional damage, have been obtained. Further, here we found a simple property of the incipient full sliding relative microdisplacements

$$\delta_{\max} = f g_{\max},$$

where f is the friction coefficient and $g_{\max}$ is the maximum gap of the unloaded profiles. This result, together with simplified FF criteria based on microdisplacement, provides a very simple mean for designers to compare different geometrical choices, simply finding the contact area dimension from the analytical formulae, also provided here. A straightforward extension for frictional damage reads

$$D_{\max} = f[p(x)g(x)]_{\max},$$

which needs only the additional effort to compute the pressure distribution, again analytically given here. Further, $D_{\max}$ is shown to have a weak dependence on geometry, and a parameter $D_0 = 8/\pi(fp_m)^2 A/\pi b$ is introduced which gives once again a quick reference for the designer. Both criteria $\delta_{\max}$, $D_{\max}$ have also the merit to point out the critical importance of the friction coefficient (linear dependence for $\delta_{\max}$, quadratic for $D_{\max}$), which is known to 'unfortunately' increase significantly during the fretting process – more precise understanding of this phenomenon is actually one of the most pressing tasks for future studies.

Therefore, the present paper indicates that, by varying the radius and also the overall size of the indenter with respect to the *intrinsic* material defect size, the effect of stress concentration and frictional damage

should be separated efficiently, so that experiments along this direction should finally shed some light into the problem. Recent experimental investigations seem to indicate a better FF behavior with smaller punch radius, which is quite surprising for fatigue design engineers. However, it is not clear whether this benefit continues up to a vanishing small radius, or there is the "optimal" radius corresponding to the maximum of FF life. This, together with variations on the geometry of the dovetail joint, particularly removing tension from the fretted regions, should result in optimal designs. In any case, the rounded flat geometry proves to be a preferred vehicle for both exploring a complex area intermediate between classical fatigue and fracture mechanics, and also improves the FF performance of dovetail joints.

Acknowledgements

Michele Ciavarella is pleased to acknowledge the support from CNR-Consiglio Nazionale delle Ricerche for support of the February–August 1998 and the July 1999 visits to the Oxford University, permitting different stages of completion of the present work. Discussion with Dr. Roy Moobola, Dr. David Nowell and Prof. David Hills in Oxford, and support from CNR for the network COMES (Computational Mechanics of Solids) at CNR-IRIS are also acknowledged.

References

Archard, J.F., 1957. Elastic deformation and the laws of friction. Proc. R. Soc. Lond. A 243, 190–205.

Araujo, J.A., Nowell, D., 1999. Analysis of pad size effects in fretting fatigue using short crack arrest methodologies. Int. J. Fat. 21 (9), 947–956.

Ballard, P., Dan Van, K., Deperrois, A., Papadaopoulos, Y.V., 1995. High cycle fatigue and a finite element analysis. Fat. Fract. Engng. Mat. Struct. 18 (3), 397–411.

Bower, A.F., Johnson, K.L., 1989. The influence of strain-hardening on cumulating plastic deformation in rolling and sliding contact. J. Mech. Phys. Solids 37 (4), 471.

Bramhall, R., 1973. Studies in fretting fatigue. D. Phil. thesis, University of Oxford.

Cattaneo, C., 1938. Sul contatto di due corpi elastici: distribuzione locale degli sforzi. Rendiconti dell'Accademia Nazionale dei Lincei 27, 342–348, 434–436, 474–478.

Cattaneo, C., 1947a. Teoria del contatto elastico in seconda approssimazione: compressione obliqua. Rendiconti Seminario Facoltá Scienze di Cagliari, volume 17, 13–28.

Cattaneo, C., 1947b. Compressione Obliqua 17, 13–28.

Ciavarella, M., 1998a. The generalized Cattaneo partial slip plane contact problem. Theory. Int. J. Solids Struct. 35 (18), 2349–2362.

Ciavarella, M., 1998b. The generalized Cattaneo partial slip plane contact problem. Examples. Int. J. Solids Struct. 35 (18), 2363–2378.

Ciavarella, M., 1998c. Tangential loading of general 3D contacts. J. Appl. Mech. 64(4), 998–1003.

Ciavarella, M., 1999. Indentation by nominally flat or conical indenters with rounded Corners. Int. J. Solids Struct. 36 (27), 4149–4181.

Ciavarella, M., Demelio, G., 1999. On non-symmetrical plane contacts. Int. J. Mech. Sci. 41 (12), 1533–1550.

Ciavarella, M., Demelio, G., Hills, D.A., 1999a. The use of almost complete contacts for fretting fatigue tests. In: Panontin, T.L., Sheppard, S.D. (Eds.), Fatigue and Fracture Mechanics, vol. 29. ASTM STP 1332, American Society for Testing and Materials, West Conshohocken, PA, pp. 696–709.

Ciavarella, M., Demelio, G., Hills, D.A., 1999b. An analysis of rotating bending fretting fatigue tests using 'bridge' specimens. In: Hoeppner, D.W., Chandrasekaran, V., Elliot, C.B. (Eds.), Fretting Fatigue: Current Technologies and Practices. ASTM STP 1367. American Society for Testing and Materials, West Conshohocken, PA.

Ciavarella, M., Demelio, G., Jang, Y.H., Barber, J.R., 2000. Linear elastic contact of the Weierstrass profile. Proceedings of the Royal Society, Series A 456 (N1994), 387–405.

Ciavarella, M., Hills, D.A., Monno, G., 1998. The influence of rounded edges on indentation by a flat punch. Inst. Mech. Engng. part C – J. Mech. Engng. Sci. 212 (4), 319–328.

Ciavarella, M., Hills, D.A., 1999. Brief note: some observation on oscillating tangential forces and wear in general plane contacts. Eur. J. Mech. A: Solids 18, 491–497.

Ciavarella, M., Hills, D.A., Moobola, R., 1999. Analysis of plane, rough contacts, subject to a shearing force. Int. J. Mech. Sci. 41 (1), 107–120.

Collins, J.A., Tovey, F.M., 1972. Fretting fatigue mechanisms and the effect of direction of fretting motion on fatigue strength. J. Mater. JMSLA 7 (4), 1–15.

Dai, D.N., Nowell, D., 1998. Analysis of surface tractions in complex fretting fatigue cycles using quadratic programming. J. Trib. ASME 120 (4), 744–749.

Eden, E.M., Rose, W.N., Cunningham, F.L., 1911. The endurance of metals. Proc. Inst. Mech. Engrs. 875, 68–76.

Edwards, P.R., 1981. The application of fracture mechanics to predicting fretting fatigue. In: Waterhouse, R.B. (Ed.), Fretting Fatigue. Applied Science Publishers, London, pp. 67–98.

Endo, K., Goto, H., 1976. Initiation and propagation of fretting fatigue cracks. Wear 38, 311–324.

Fellows, L.J., Nowell, D., Hills, D.A., 1995. Contact stresses in a moderately thin strip with particular reference to fretting experiments. Wear 185 (1,2), 235–238.

Fellows, L.J., Nowell, D., Hills, D.A., 1997. Analysis of crack initiation and propagation in fretting fatigue: The effective initial flaw size methodology. Fatigue Fract. Engng. Mat. Struct. 20 (1), 61–70.

Fenner, A.J., Wright, K.H.R., Mann, J.Y., 1956. Fretting corrosion and its influence on fretting failure. Proc. Int. Conf. on fatigue of Metals. Institute for Mechanical Engineers, London, p. 368.

Fouvry, S., Kapsa, P., Sidoroff, F., Vincent, L., 1998. Identification of the characteristic length scale for fatigue cracking in fretting contacts. J. de Phys. IV 8 (P8), 159–166.

Giannakopoulos, A.E., Lindley, T.C., Suresh, S., 1998. Overview No.129, Aspects of equivalence between contact mechanics and fracture mechanics: theoretical connections and a life-prediction methodology for fretting-fatigue. Acta mater. 46 (9), 2955–2968.

Gillet, H.M., Mack, E.L., 1924. Notes on some endurance tests of metals. Proc. Am. Soc. Test. Mat. 24, 476.

Hills, D.A., Nowell, D., 1992. The development of a fretting fatigue experiment with well-defined characteristics. In: Attia, M.H., Waterhouse, R.B. (Eds.), Standardization of Fretting Fatigue Test Methods and Equipment. ASTM STP, ASTM, Baltimore, 1159, pp. 69–84.

Hills, D.A., Nowell, D., 1994. Mechanics of fretting fatigue. Kluwer, Dordrecht.

Hills, D.A., Nowell, D., Sackfield, A., Mechanics of elastic contacts, Butterworth–Heinemann, Oxford, 1993.

Hills, D.A., Sosa, G.U., 1999. Origins of partial slip in fretting – a review of known potential solutions. J. Strain Anal. 34 (3), 175–181.

Hills, D.A., Kelly, P.A., Dai, D.N., Koronsky, A.M., 1996. Solution of crack problems: the distributed dislocation technique, Kluwer Academic Publishers, Dordrecht.

Hoeppner, 1994. D.W., Mechanisms of fretting fatigue, ESIS 18. In: Waterhouse, R.B., Lindley, T.C. (Eds.), Mechanical Engineering Publications, London, pp. 3–19.

Hoeppner, D.W., Gates, F.L., 1981. Fretting fatigue considerations in engineering design. Wear 70, 155–164.

Hutson, A.L., Nicholas, T., Goodman, R, 1999. Fretting fatigue of Ti-6Al-4V under flat-on-contact. Int. J. Fat. 21, 663–669.

Iyer, K., Mall, S., 1999. Analyses of contact pressure and stress amplitude effects on fretting fatigue life. ASME J. Engng. Mat. Tech., in press.

Jaeger, J., 1998. A new principle in contact mechanics. ASME J. Trib. 120 (4), 677–684.

Kuno, M., Waterhouse, R.B., Nowell, D., Hills, D.A., 1989. Initiation and growth of fretting fatigue cracks in the partial slip regime. Fat. Fract. Engng. Mater. Struct. 12 (5), 387–398.

Lindley, T., 1997. Fretting fatigue in engineering alloys 19 (Suppl.1), S39–S49.

McDowell, J.R., 1953. Fretting Corrosion. STP, Philadelphia, PA, ASTM, 144, pp. 24–39.

Mindlin, R.D., 1949. Compliance of elastic bodies in contact. J. Appl. Mech. 16, 259–268.

Moobola, R., Hills, D.A., Nowell, D., 1998. Designing against fretting fatigue: crack self-arrest. J. Strain Anal. 33 (1), 17–25.

Moobola, R., 1998. Aspects of initiation and self-arrest fretting fatigue. D. Phil. thesis, University of Oxford.

Munisamy, R.L., Hills, D.A., Nowell, D., 1995. An analysis of coupling between plane contacts and cracks. Eur. J. Mech. part A: Solids 14 (1), 985–991.

Neu, R.W., Pape, J.A., Swalla, D.R., 1999. Methodologies for linking nucleation and propagation approaches for predicting life under fretting fatigue. In: Hoeppner, D.W., Chandrasekaran, V., Elliot, C.B. (Eds.), Fretting Fatigue: Current Technologies and Practices, ASTM STP 1367. American Society for Testing and Materials, West Conshohocken, PA.

Nishioka, K., Nishimura, S., Hirakawa, K., 1968. Fundamental investigation of fretting fatigue, part 1. On the relative slip amplitude of press-fitted axle assemblies. Bull. JSME 11, 437–445.

Nishioka, K., Hirakawa, K., 1969a. Fundamental investigation of fretting fatigue, part 3. Some phenomena and mechanism of surface cracks. Bull. JSME 12, 397–407.

Nishioka, K., Hirakawa, K., 1969b. Fundamental investigation of fretting fatigue, part 4. The effect of mean stress. Bull. JSME 12, 408–414.

Nishioka, K., Hirakawa, K., 1969c. Fundamental investigation of fretting fatigue, part 5. The effect of relative slip amplitude. Bull. JSME 12, 692–697.

Nix, K.J., Lindley, T.C., 1985. The application of fracture-mechanics to fretting fatigue. Fat. Fract. Engng. Mat. Struct. 8 (2), 143–160.

Nowell, D., 1988. An analysis of fretting fatigue. D. Phil. thesis, University of Oxford.

Nowell, D., Hills, D.A., 1990. Crack initiation criteria in fretting fatigue. Wear 136, 329–343.

Pape, J.A., Neu, R.W., 1999. Influence of contact configuration in fretting fatigue testing. Wear 229 (2), 1205–1214.
Ruiz, C., Buddington, P.H.B., Chen, K.C., 1984. An investigation of fatigue and fretting in a dovetail joint. Exp. mech. 24 (3), 208–217.
Ruiz, C., Chen, K.C., 1986. Life assessment of dovetail joints between blades and discs in aero-engines. Proc. Int. Conf. Fatigue, Sheffield. Institute for Mechanical Engineers, London.
Szolwinski, M.P., Farris, T.N., 1996. Mechanics of fretting fatigue crack formation. Wear 198 (1,2), 93–107.
Szolwinski, M.P., Farris, T.N., 1998. Observation, analysis and prediction of fretting fatigue in 2024-T351 aluminum alloy. Wear 221, 24–36.
Taylor, D., 1999. Geometrical effects in fatigue: a unifying theoretical model. Int. J. Fat. 21, 413–420.
Thomson, D., 1998. The national high cycle fatigue (HCF) program. In: Strange, W.A. (Ed.), Third Nat. Turbine Engine High Cycle Fatigue conference, Saint Antonio, TX, CDRom proceedings.
Tomlinson, G.A., 1927. The rusting of steel surfaces in contact. Proc. Roy. Soc. Lond. A 115, 472–483.
Warlow-Davis, E.J., 1941. Fretting corrosion and fatigue strength: Brief results of preliminary experiments. Proc. Inst. Mech. Engrs. 146, 32.
Waterhouse, R.B., 1981. Fretting fatigue. Applied Science Publishers, London.
Waterhouse, R.B., 1992. Fretting fatigue. Int. Mat. Rev. 37 (2), 77–97.
Waterhouse, R.B., Lindley, T., 1993. Proc. of the Int. Conf. Fretting Fatigue, Sheffield, 1993, MEP, London.
Wright, T., O'Connor, J.J., 1972. The influence of fretting and geometric stress concentrations on the fatigue strength of clamped joints, vol. 186. Proc. Instn. Mech. Engrs., p. 827.
Zhou, Z.R., Vincent, L., 1999. Lubrication in fretting – a review. Wear 229 (2), 962–967.